ISSN 1028-334X, Doklady Earth Sciences, 2007, Vol. 412, No. 1, pp. 106–109. © Pleiades Publishing, Ltd., 2007.
Original Russian Text © S.A. Bushmin, D.V. Dolivo-Dobrovolsky, Yu.M. Lebedeva, 2007, published in Doklady Akademii Nauk, 2007, Vol. 412, No. 3, pp. 383–387.

GEOCHEMISTRY

Infiltration Metasomatism under High-Pressure Granulite-Facies Conditions Based on Orthopyroxene–Sillimanite Rocks in Shear Zones of the Lapland Granulite Belt

S. A. Bushmin, D. V. Dolivo-Dobrovolsky, and Yu. M. Lebedeva

Presented by Academician D.V. Rundqvist, February 28, 2005

Received February 28, 2006

DOI: 10.1134/S1028334X07010242

The influx of mantle fluids is an important process affecting the evolution of the granulite complex. Some researchers suggest that these fluids in the granulite areas consisted mainly of CO_2 with insignificant content and low activity of H_2O [10]. However, H_2O-depleted fluids can hardly promote infiltration metasomatism with significant transfer of major components in granulites. Recent theoretical and experimental studies showed that, at high *PT* parameters of the granulite-facies level, fluids can be significantly hydrous with a low activity of water owing to the high salinity of fluids at moderate and fairly high pressures [11, 14, 15].

Specific features of the geology and petrology of orthopyroxene–sillimanite rocks confined to the shear zone with intense blastomylonitization in the southeastern part of the Lapland granulite belt (LGB) testify to the intense filtration of essentially hydrous fluids similar to those proposed in [15, 11, 14], which fostered metasomatic redistribution and transportation of major elements. The fluids were hydrous enough to dissolve, transport, and redeposit the major elements. This is supported by specific features, such as distinct spatial differentiation of the matter expressed in intense silicification, as well as the development of quartz veins and lenticular veins of monomineral, bimineral, and low-mineral rocks sharply enriched in individual elements. Since the high-pressure infiltration processes are poorly studied, the quantitative precise assessment of their *PT* conditions is a pressing issue.

Institute of Precambrian Geology and Geochronology, Russian Academy of Sciences, nab. Makarova 2, St. Petersburg, 199034 Russia;
e-mail: bushmin@sb1402.spb.edu

Geology of the area. The southeastern termination of LGB in the southern Kola Peninsula is represented by the Por'ya guba granulites. The study region has a scaly structure owing to overthrusting of granulite aluminous gneisses of the Umba suite onto the orthopyroxene and two-pyroxene schists and gneisses of the Por'ya Guba. At present, rock blocks of the region are represented by a package of slices (Fig. 1). Overthrusting and formation of a large melange zone (~1.9 Ga) in early granulites (1.92–1.96 Ga) produced the NW-trending blastomylonite zones [1], where intense plastic and brittle deformations occurred under conditions of repeated granulite- and amphibolite-facies metamorphism.

Geology of orthopyroxene–sillimanite rocks. High-Mg orthopyroxene–sillimanite rocks formed during blastomylonitization in a shear zone at the northeastern margin of the Por'ya Guba granulite block near the melange zone (Fig. 1). Some researchers consider these rocks products of isochemical metamorphism [5, 7, 9], while others believe that they are metasomatites [2, 4].

Rocks with the orthopyroxene–sillimanite assemblage were found only in three sites confined to Palenyi Island and the Gorelyi Island area within a NW-trending blastomylonite zone 100 m wide (Palenyi Island) and about 15 km long. The temporal relation of orthopyroxene–sillimanite assemblages with deformations in the shear zone was proved by microtextural studies [7]. On Palenyi Island, the zone with these rocks is located among clinopyroxene, two-pyroxene (±biotite, hornblende), and orthopyroxene (±biotite) crystalline schists of mafic and intermediate compositions with intercalations of orthopyroxene plagiogneisses. Migmatized garnet-bearing varieties of pyroxene crystalline schists and plagiogneisses predominate near and inside the shear zone at the contact with orthopyroxene–sillimanite rocks.

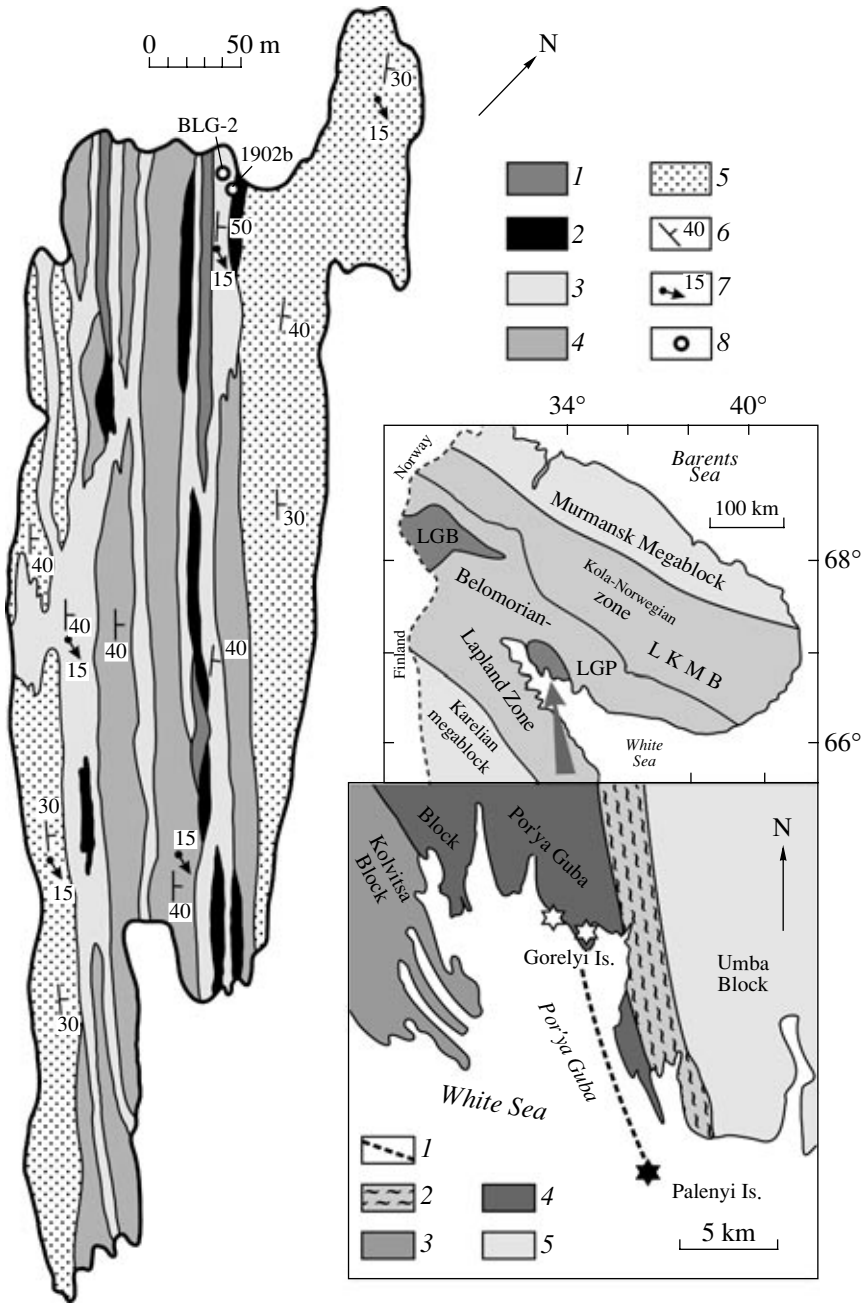

Fig. 1. Geological scheme of the development area of orthopyroxene–sillimanite and related rocks among the granulites of Palenyi Island, Por'ya Guba. Compiled by S.A. Bushmin and Yu.M. Lebedeva with the application of data in [8]. (*1*) Scapolite–plagioclase and scapolite–diopside rocks; (*2*) coarse- and medium-grained garnet–orthopyroxene rocks with variable content of sillimanite, quartz, cordierite, spinel, and sapphirine; (*3*) sillimanite quartzites and quartz-rich rocks with sillimanite, orthopyroxene, garnet, cordierite, biotite, spinel, and sapphirine and pockets of sulfide mineralization; (*4*) garnet-bearing pyroxene crystalline schists and gneisses; (*5*) orthopyroxene and two-pyroxene crystalline schists and gneisses with patches of migmatites and granite gneisses; (*6*) foliation and mylonitic banding; (*7*) lineation; (*8*) sampling site. Legend for the upper inset: (LGB) Lapland granulite belt; (LKMB) Lapland–Kola mobile belt. Legend for the lower inset: (*1*) blastomylonite zone with orthopyroxene–sillimanite rocks, (*2*) tectonic melange zone; (*3*) gabbro anorthosites; (*4*) orthopyroxene and two-pyroxene crystalline schists and gneisses; (*5*) aluminous gneisses and felsic granulites.

Mineral composition of the rocks. In some places, the orthopyroxene–sillimanite rocks are formed during the alteration of pyroxene crystalline schists. However, the primary rocks are more often represented by weakly migmatized orthopyroxene and garnet–orthopyroxene gneisses (in Grt: X_{Mg} = 0.45–0.59, X_{Ca} = 0.17–0.20; in Opx: X_{Mg} = 0.60–0.63, Al = 0.20–0.22).*

* Mineral abbreviations are as in [10]. In Grt, X_{Mg},Ca = Mg, Ca/(Mg + Fe + Mn + Ca); in Opx, Crd, and Bt, X_{Mg} = Mg/(Mg + Fe); in Bt, X_{Al} = Al/(Al + Si); in Opx, Al is given in f.u.

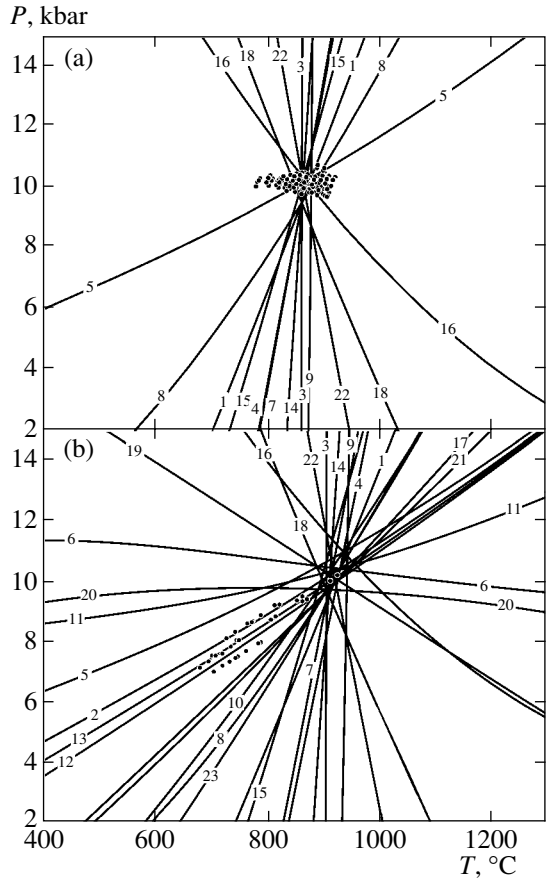

1 – Alm = *Al*-Opx + 3Fs,
2 – 3β-Qtz + Grs + 2Alm = 3An + 6Fs,
3 – 3Fs + Phl = 3En + Ann,
4 – 3En + Alm = 3Fs + Prp,
5 – β-Qtz + Alm = 3Fs + Sil,
6 – 3β-Qtz + Grs + 2*Al*-Opx = 3An,
7 – Phl + Alm = *Al*-Opx + Ann + 3En,
8 – Prp = Al-Opx + 3En,
9 – Sil = Al-Opx + β-Qtz,
10 – 2Alm + Grs + 2Phl + 3β-Qtz = 6En + 3An + 2An + 2Ann,
11 – Grs + 2Prp + 3β-Qtz = 6En + 3An,
12 – 3Sil + Grs + 3Fs = Alm + 3An,
13 – Grs + β-Qtz + 2Sil = 3An,
14 – Alm + Phl = Prp + Ann,
15 – β-Qtz + Phl + Alm = Ann + 3En + Sil,
16 – Prp + β-Qtz = Sil + 3En,
17 – Grs + 3Sil = 3An + *Al*-Opx,
18 – Prp + Ann = *Al*-Opx + 3Fs + Phl,
19 – 3β-Qtz + 2Prp + Grs + 2Ann = 3An + 6Fs + 2Phl,
20 – 3Sil + 3En + Grs + Ann = Alm + 3An + Phl,
21 – 3Sil + 3En + Grs = 3An + Prp,
22 – β-Qtz + Prp + Ann = 3Fs + Phl + Sil,
23 – 3Sil + Phl + Grs + 3Fs = Ann + 3An + Prp.

Fig. 2. Results of thermobarometric study of the orthopyroxene–sillimanite rocks by the TWEEQU method (thermodynamic dataset [13]). Equilibrium curves correspond to *PT* determinations demonstrating least mean square deviations of intercepts (MSD). Data points show the remaining determinations in the indicated samples. (LIE) quantity of linearly independent equilibria. (a) Sample BLG-2, 4 LIE, T = 870°C (MSD = 9°), P = 10.05 kbar (MSD = 0.44 kbar); (b) sample 1902b, 5 LIE, T = 924°C, (MSD = 24°), P = 10.22 kbar (MSD = 0.51 kbar).

The orthopyroxene–sillimanite rocks are dominated by quartz-rich Al–Si–Mg rocks and quartzites with sillimanite, high-Mg orthopyroxene and garnet, plagioclase, K-feldspar, and late cordierite and biotite. The rocks have a spotty–banded, occasionally thin-banded structure, which is typical of blastomylonites with "striated" distribution of minerals. The rocks have a heterogeneous structure with distinctly zoned distribution of minerals and the formation of polymineral to monomineral zones. Zoning is represented by different assemblages with the number of minerals gradually decreasing in the course of their sequential replacement and dissolution (leaching) up to the formation of garnet–orthopyroxene–sillimanite rocks (in Grt, X_{Mg} = 0.57–0.68; in Opx, X_{Mg} = 0.76–0.81, Al = 0.36–0.42), garnet–sillimanite rocks (in Grt, X_{Mg} = 0.60–0.66), orthopyroxene–sillimanite rocks (in Opx, X_{Mg} = 0.77–0.79, Al = 0.37–0.40), and sillimanite quartzites with quartz and sillimanite clots. Quartzites with orthopyroxene and garnet contain spinel grains at the contact with quartz.

Silicified and quartz orthopyroxene–sillimanite rocks are spatially associated with compositionally diverse base- and alkali-rich (Fe, Mg, Ca, Na, K) porphyroblastic and veined rocks: sillimanite–orthopyroxene–garnet (in Grt, X_{Mg} 0.57–0.71; in Opx, X_{Mg} = 0.77–0.82, Al = 0.38–0.39) and sillimanite–cordierite–orthopyroxene rocks, as well as garnet (in Grt, X_{Mg} = 0.39–0.44), scapolite–diopside, sillimanite–diopside, biotite–orthopyroxene, and K feldspar–biotite rocks.

Sillimanite-bearing orthopyroxene rocks of both Al–Si and Fe–Mg compositions contain magnesian cordierite (X_{Mg} = 0.87–0.93), which crystallized as independent grains during metasomatism or was involved in formation of mineral rims and symplectites. Late orthopyroxene–cordierite symplectites are observed around both matrix garnet and earlier orthopyroxene–sillimanite symplectite intergrowths. Late magnesian biotite (X_{Mg} = 0.82–0.94, X_{Al} = 0.32–0.33) forms separate clots, small linear zones, and veinlets.

Reaction structures with orthopyroxene and sillimanite. The specific features of mineral zoning, the constitution of minerals and their replacements, and reaction structures in the orthopyroxene–sillimanite rock bodies indicate that they were formed mainly by

infiltration metasomatism with the output (leaching)/input (redeposition) of major elements, i.e., allochemical (metasomatic) mineral reactions. These reactions are expressed in structures of dissolution, replacement, and crystallization of matrix minerals; the appearance of branching veinlets; and porphyroblastesis with significant changes in the mineral content.

Breakdown of the high-Mg matrix garnet with the formation of symplectite played a subordinate role in the formation of the orthopyroxene + sillimanite assemblage. Garnets with different Mg contents are replaced by symplectites with different orthopyroxene compositions:

$$\text{Grt } (X_{Mg} = 0.65\text{–}0.68)$$
$$\rightarrow \text{Opx}(X_{Mg} = 0.83\text{–}0.84, \quad \text{Al} = 0.32\text{–}0.38) + \text{Sil},$$
$$\text{Grt } (X_{Mg} = 0.58\text{–}0.61)$$
$$\rightarrow \text{Opx}(X_{Mg} = 0.78\text{–}0.80, \quad \text{Al} = 0.26\text{–}0.37) + \text{Sil}.$$

Occasionally, symplectites replacing garnet (X_{Mg} = 0.57–0.60) contain inclusions of Mg-rich garnet (X_{Mg} = 0.61–0.65) and sapphirine (X_{Mg} = 0.87). One can also see veins composed of coarse-grained intergrowths of orthopyroxene, sillimanite, quartz, and occasional K-feldspar.

PT conditions. The presence of the spinel + quartz assemblage in garnet–orthopyroxene–sillimanite quartzites, which do not yet contain orthopyroxene–sillimanite symplectites and late cordierite, attests to extremely high temperatures (about 900°C or more) at pressures about 10 kbar [6]. This confirms the *PT* estimates of the orthopyroxene–sillimanite rocks obtained by the TWEEQU method [12]. The garnet–orthopyroxene–sillimanite–quartz rock (with plagioclase and biotite) from leaching zone defines T = 870°C and P = 10.1 kbar (Fig. 2, sample BLG-2), while sillimanite–orthopyroxene garnet rock (with quartz, plagioclase, and biotite) at the contact with leaching zone yields T = 924°C and P = 10.2 kbar (Fig. 2, Sample 1902b) [2].

Thus, intense infiltrational metasomatic processes related to the influx of high-temperature fluids had already begun during thrusting at peak temperatures and pressures (870–924°C and 10.1–10.2 kbar), which were significantly higher than the *PT* parameters of the previous stage of granulite metamorphism (T = 740–800°C, P = 6–7.5 kbar) [3]. Orthopyroxene–sillimanite symplectites formed at decreasing temperature and/or pressure are widespread in rocks that yet lack late orthopyroxene–cordierite symplectites (indicator of significant decompression). Hence, the evolution of shear zones was accompanied by both cooling and pressure drop. The replacement of early matrix minerals in the orthopyroxene–sillimanite rocks by later symplectite coronas reflects a significant decrease in the intensity of fluid flow and/or a lack of water fluid, with diffusion-controlled crystallization from weakly mobile fluid at a high level of system disequilibrium during the late stage of mineral formation (granulite-facies metamorphism) in the shear zones.

ACKNOWLEDGMENTS

This work was supported by the Federal Program for the Support of Leading Scientific Schools (project no. 4732.2006.05).

REFERENCES

1. V. V. Balagansky and V. A. Glebovitsky, in *Early Precambrian of the Baltic Shield* (Nauka, St. Petersburg, 2005), pp. 127–175 [in Russian].
2. O. A. Belyaev, in *Metasomatism and Metasomatites in the Precambrian Metamorphic Complexes* (Kol'sk. Fil. Akad. Nauk SSSR, Apatity, 1981), pp. 10–19 [in Russian].
3. O. A. Belyaev and V. P. Petrov, in *Metamorphic Facies of the Eastern Baltic Shield* (Nauka, Leningrad, 1990), pp. 20–27 [in Russian].
4. S. A. Bushmin, L. V. Kuleshevich, and V. V. Severin, in *Metamorphic Facies of the Eastern Baltic Shield* (Nauka, Leningrad, 1990), pp. 87–118 [in Russian].
5. V. A. Glebovitsky, N. L. Alekseev, and D. V. Dolivo-Dobrovolsky, Zap. Vseross. Mineral. O–va, No. 2, 1 (1997).
6. K. K. Podlesskii, Dokl. Earth. Sci. **389**, 248 (2003) [Dokl. Akad. Nauk **389**, 84 (2003)].
7. N. E. Kozlova, V. V. Balagansky, et al., Izv. Akad. Nauk SSSR, Ser. Geol., No. 4, 66 (1991).
8. M. D. Krylova, *Geological–Geochemical Evolution of the Lapland Granulite Belt* (Nauka, Moscow, 1983) [in Russian].
9. M. D. Krylova and L. A. Priyatkina, Dokl. Akad. Nauk SSSR **226**, 661 (1976).
10. L. L. Perchuk and T. V. Gerya, in *Experimental Mineralogy* (Nauka, Moscow, 2004), Vol. 2, pp. 137–157 [in Russian].
11. L. Y. Aranovich and R. C. Newton, Contrib. Mineral. Petrol. **125**, 200 (1996).
12. R. G. Berman, Can. Mineral. **29**, 833 (1991).
13. R. G. Berman and L. Ya. Aranovich, Contrib. Mineral. Petrol. **126**, 1 (1996).
14. R. C. Newton, L. Ya. Aranovich, E. C. Hansen, et al., Precambrian Res. **38**, 21 (1998).
15. K. I. Shmulovich and C. M. Graham, Contrib. Mineral. Petrol. **124**, 376 (1996).